Simple model for river network evolution

Robert L. Leheny
The James Franck Institute and the Department of Physics, The University of Chicago, 5640 South Ellis Avenue, Chicago, Illinois 60637
(Received 28 April 1995)

We simulate the evolution of a drainage basin by erosion from precipitation and avalanching on hillslopes. The avalanches create a competition in growth between neighboring basins and play the central role in driving the evolution. The simulated landscapes form drainage systems that share many qualitative features with Glock's model for natural network evolution and maintain statistical properties that characterize real river networks. We also present results from a second model with a modified, mass conserving avalanche scheme. Although the terrains from these two models are qualitatively dissimilar, their drainage networks share the same general evolution and statistical features.

PACS number(s): 02.70.−c, 07.05.Tp, 92.40.Fb, 92.40.Gc

I. INTRODUCTION

A general understanding of the driving mechanisms for pattern formation in nature remains incomplete. Recently, river networks have emerged as a model dynamical system to study these issues. The basis of this research has been to identify the underlying sources for the numerous statistical laws relating different features of drainage networks. In a closely related area of research, geomorphologists have developed a qualitative picture of the characteristic evolution that these networks experience. The extremely long time scales for this evolution, however, have greatly restricted the opportunities for direct observation of temporal changes, and further understanding of the process has relied on the inference of an age sequence to groups of river networks selected from different locations. Consequently, few studies have successfully related the evolution of drainage basins to their statistical properties.

The numerous efforts to model river networks have primarily focused on reproducing the statistical characteristics rather than the temporal behavior of natural networks. One popular approach involves modeling rivers as random-walk paths drawn on a two-dimensional lattice, each path continuing until it joins a previous path or reaches the lattice boundary [1,2]. The resulting branched patterns simulate the structure of river networks, and the degree of success each model has in reproducing natural networks' statistical features depends on the specific rules dictating the random-walk paths [3]. Other models [4–9] offer variations on the random-walk procedure, such as the headward growth of walk patterns, and these simulations have reproduced many of the statistical characteristics of natural river systems with reasonable success. However, this success has been criticized as "illusory" [10]. Since river networks constitute extremely complex systems where many factors vary independently both spatially and temporally, a network's response to this multitude of variations appears well simulated by a random variable [6]. Abrahams [10] has argued that none of the random-walk simulations offer insight into the geomorphic processes that determine network evolution.

Recently, the idea that drainage basins may be an example of a self-organized critical state has led to the study of network formation in terms of the attainment of features which reveal critical scaling. Following an approach similar to that developed by Howard [11], Rodríguez-Iturbe *et al.* [12] have postulated that river networks arrange themselves to minimize their energy expenditure, and they have compared the networks modeled on this assumption with natural systems [13]. Similarly, Inaoka and Takayasu [14] have presented a model in which erosion drives a landscape with random roughness to a final state where the water is channeled into a network of rivers. The fully developed networks in each of these models are static structures with spatial features that show critical scaling and share statistical properties with natural rivers. However, real drainage basins are not static but proceed through a characteristic evolution on geological time scales. Therefore, one can ask how river networks maintain their statistical properties as they evolve in time.

Clearly, to understand the important mechanisms affecting a river network's evolution one must consider its interaction with the surrounding landscape. Two new physical models address this issue. In these models continuum equations, solved discretely on a lattice, describe landscape changes due to a variety of erosional processes. Willgoose *et al.* [15] have modeled the development of a drainage network that, initialized at the edge, grows by erosion to extend throughout the lattice. The rivers, once present at a lattice site, remain fixed there. However, the resulting physically realistic depiction of network initiation has allowed them to trace the temporal behavior of a variety of network statistics during this growth period [16]. Following a similar strategy, but with a different set of continuum equations, Howard [17] has simulated the transformation of a rough surface as it establishes a channeled drainage pattern through a process of retreating hillslopes and fluvial erosion.

While these physical models make a comprehensive

effort to describe the relevant processes in drainage basin evolution, their complexity limits the size of feasible simulations (the largest simulation in either study contained 10^4 lattice sites) and correspondingly compromises the resolution of network and landscape features. Our simulations of landscape erosion and drainage network evolution apply a different approach. We have developed a model whose rules are as simple as possible but which nonetheless produces rich spatial and temporal behavior. Maintaining simplicity allows us to identify unambiguously the sources of the dynamics in the simulations and their consequences. Examining both the model's successes and limitations provides insight into mechanisms capable of producing various river network properties.

A central feature of the model is an avalanche scheme which produces a realistic hillslope development and drives a competition in growth between neighboring drainage basins. Recent experiments have highlighted the importance of avalanching for the production of landscape features seen in nature [18]. Our study concentrates on the temporal behavior of the landscapes' associated river networks, and we find that the networks maintain many of the statistical characteristics familiar to natural systems during their evolution. In a previous report we summarized a version of the model in which avalanched mass is not conserved and described some of its results [19]. Because of the importance of avalanches in driving the network evolution, we have extended our investigation to a model with an alternative, mass conserving avalanche scheme. The contrasting behaviors of the two models provide insight into the role conserved variables play in this dynamical system. In this paper we provide a comprehensive analysis of the features of the drainage networks that the original model produces, and compare our findings with results from this new, mass conserving model.

II. MODEL FOR NETWORK EVOLUTION

A. The rules

In the model a rectangular lattice of points describes an eroding terrain with the height of the land, $h(x,y)$, specified at each point. The lattice has periodic boundary conditions in the x direction:

$$h(x,y)=h(x+W,y) . \tag{1}$$

The simulation begins with the landscape as a featureless incline:

$$h(x,y)=Iy , \tag{2}$$

where I is the initial slope. The terrain changes from the effects of a single precipitation event at each iteration according to the following procedure.

(i) Precipitation lands at a random site on the lattice.

(ii) The water flows from the site it occupies to one of four nearest neighbors until it reaches the lattice edge, $y=0$. The probability distribution that determines to which neighbor the water flows is

$$P(\Delta h_i)=\begin{cases}\exp(E\Delta h_i)\left[\displaystyle\sum_{j=1,\Delta h_j\geq 0}^{j=4}\exp(E\Delta h_j)\right]^{-1}, & \Delta h_i\geq 0 ,\\ 0, & \Delta h_i<0 ,\end{cases} \tag{3}$$

where Δh_i is the height of the occupied site minus the height of the neighbor i, and E is a free parameter in the model. We choose $E<1/I$ so that precipitation on the initial slope has nearly equal probability to move in either the x direction or toward $y=0$. This exponential dependence directs the water down steep slopes it encounters, but allows it to take a meandering path on the initial slope, thus accounting for topographic features on scales finer than any set by model parameters and introducing randomness to the otherwise pristine initial slope.

(iii) Once the water reaches $y=0$, each lattice point (x,y) that it has visited loses D units of height to simulate the water's erosion:

$$h(x,y)\rightarrow h(x,y)-D . \tag{4}$$

This procedure for removing soil, which ignores both limits to the sediment carrying capacity of the precipitation and possible variations in its erosive strength, represents the simplest possible erosion process. Consequences of its simplicity become clear in our description below of the simulated landscapes.

(iv) Following the erosion, the values of Δh in the landscape are compared against a critical value, M. If any site differs in height from any nearest neighbor by more than M, then the higher site (x_h,y_h) loses $\Delta h/4$ units to simulate the avalanching of soil:

$$h(x_h,y_h)\rightarrow h(x_h,y_h)-\Delta h/4 . \tag{5}$$

In this non-mass-conserving version of the model, these units of height are simply eliminated as part of the erosion, and avalanches continue until all local slopes are less than M. In the simulations we use $M\gg D$ to limit the landscape changes from a single precipitation event. After the avalanching has completed, new precipitation enters the simulation at a random lattice point, and the process begins again at step (i).

By tracking the effects of single precipitation events of uniform strength, we avoid complications introduced by several units acting together, which may, in fact, play an important role in real drainage evolution. In this respect our model follows a qualitatively similar approach to that which Chase has developed in a lattice model for landscape erosion [20]. Chase's model incorporates a more complicated erosion scheme than we have used with a terrain smoothing, mass diffusion process. The analysis of this model has focused on relating simulated terrains' structures to natural topographical features [21].

In our simulations we can define the river networks at any time: every lattice point receives one unit of precipitation which traces a path of steepest descent, without eroding the terrain, until it reaches the lattice edge, $y=0$; all points through which at least R units flow define the river network [22]. We have examined the river patterns

formed for values of R between 20 and 1280 and find that, besides an effect on the apparent rate of network evolution and the obvious variation in drainage density, its value does not strongly influence the statistical characteristics of the river networks.

B. The terrain and river network evolution

Figures 1(a)–1(c) show a landscape formed from this model at three times in its evolution, and Figs. 1(d)–1(h) show the corresponding river networks defined at five times in the simulation. The evolution contains two distinct time scales. During the first few iterations water typically lands on an uneroded site and takes a meandering path down the initial slope before intersecting the eroded path from previous precipitation. Once it has intersected this path, if $D > I$, the probability distribution, Eq. (3), forces the water to follow it. This early aggregation process quickly forms a network of shallow incisions resembling the branching networks of random-walk models. With this pattern intact in the landscape, further evolution follows a largely deterministic process on a much longer time scale as advantageously positioned branches continue to deepen from the erosion of aggregating water and to expand their areas of influence through avalanches at the expense of neighboring branches.

The resulting evolution of the landscape and its corresponding drainage network contains many elements in common with Glock's [23] theory for the evolution of natural basins. Glock divided the evolution of a network's morphology into an early period of "extension" followed by a later period of "integration." During extension the river network experiences "elongation" by headward growth of main branches into the available land area and "elaboration" with the addition of tributary networks off of the main branches. After the network reaches maximum extension, integration begins with the "abstraction," or elimination, of small internal branches of the network as the main branches increase their own drainage area. Additional minor tributaries suffer "absorption" during integration, ceasing to exist except immediately after rainfall. A third characteristic of integration, which Glock suggested may be difficult to identify and for which no clear field evidence exists, is the aggressive adjustment of the main branches to minimize their route to the sea. Glock also noted that, simultaneous with this evolution, stream capture, or "piracy," causes major changes between networks. In stream capture a growing basin intercepts a neighboring stream and diverts it into its own network [24].

A variety of observations on natural river systems has supported Glock's model [25]. However, several of these studies [26,27] noted that the integration stage began before extension in the network was complete, as Glock indicated might occur. In addition, laboratory studies have revealed network evolution well described by Glock's model, again with pronounced temporal overlap of extension and integration [28].

In our model the headward growth and broadening of V-shaped valleys play a central role in the evolution. The terrain in Figs. 1(a)–1(c) demonstrates this headward invasion, as the valleys, initiated at the $y=0$ edge, grow to fill the available space. As they erode, the valley sides maintain flat slopes, with slope equal to $3M/4$ dictated by the avalanching. Figure 2, showing the changing cross section of the landscape in Fig. 1 at fixed y, illustrates this process. Such a parallel retreat of flat hillslopes emulates the natural maintenance of threshold, regolith covered slopes, on which the shear stability of debris dictates slope angle [29,30]. (While this headward encroachment of the river valleys into the available terrain is reminiscent of Glock's extension stage, the river patterns themselves fail to share this headward growth. The rule defining the rivers in terms of a threshold parameter, R, forces the rivers to reach within R of every

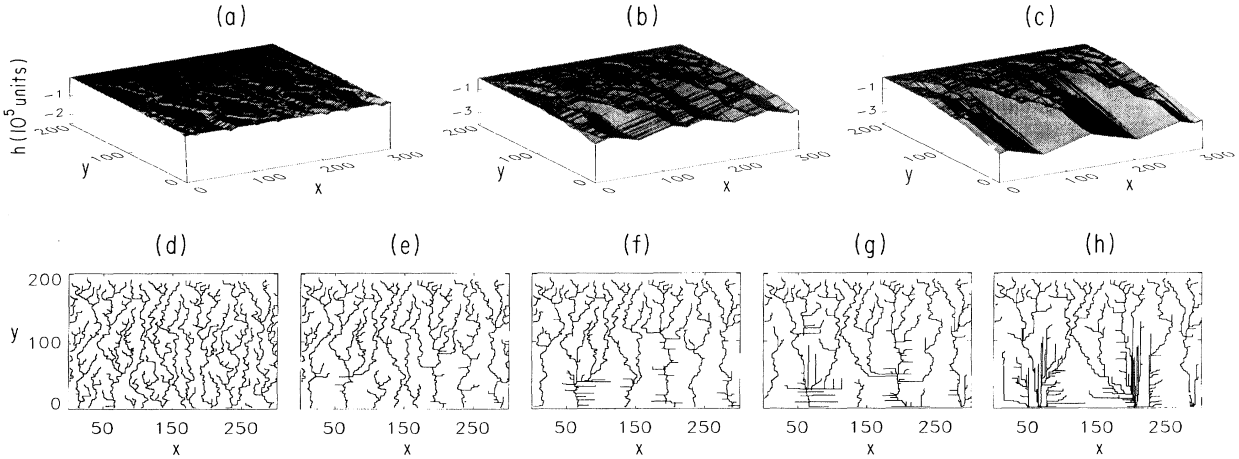

FIG. 1. The evolution of the landscape: (a) at $t=1\times10^4$ iterations, (b) at $t=5\times10^4$ iterations, and (c) at $t=9\times10^4$ iterations; and the corresponding river networks (d) at $t=1\times10^4$ iterations, (e) at $t=3\times10^4$ iterations, (f) at $t=5\times10^4$ iterations, (g) at $t=7\times10^4$ iterations, (h) at $t=9\times10^4$ iterations, in a 300×200 site simulation. The model parameters were $D=10$, $E=0.05$, $I=1.0$, $M=2000$, and $R=100$.

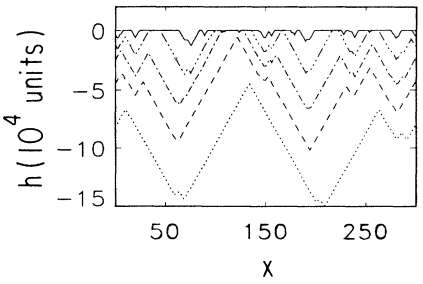

FIG. 2. Cross sections of the landscape elevation at $y=50$ in the simulation in Fig. 1: (——) at $t=1\times10^4$ iterations, (— · · · —) at $t=3\times10^4$ iterations, (—·—) at $t=5\times10^4$ iterations, (— — —) at $t=7\times10^4$ iterations, and (· · ·) at $t=9\times10^4$ iterations.

point on the lattice, so that the river networks appear at nearly full extension at very early times.)

However, the simulations follow the later patterns of natural network evolution. Internal tributaries suffer abstraction, losing their identity to the growing valleys of the main branches. In addition, stream capture occurs as the valleys of well-fed branches erode into paths of other rivers, redirecting them into the valley's branch. Figures 3(a) and 3(b), details from Figs. 1(e) and 1(f), show examples of abstraction and stream capture.

Coinciding with these changes is an increasing tendency for the main branches to straighten their paths. Figure 4, showing the distribution of the number of steps water takes without changing direction, s, as it flows through the rivers' main branches, illustrates the strong trend toward increasingly straighter paths as time increases. While Glock's prediction for this phenomenon does not include a precise description, straightening of main branches clearly plays an important role in the simulations. These features of integration that the simulations display occur as the valleys continue their headward growth, consistent with several observations of natural systems that show a pronounced temporal overlap of extension and integration.

Eventually, the valley sides of the main branches become large compared to R, and tributaries from runoff down the hillslopes appear. Figure 3(b) shows examples of these branches. Such second-generation tributaries

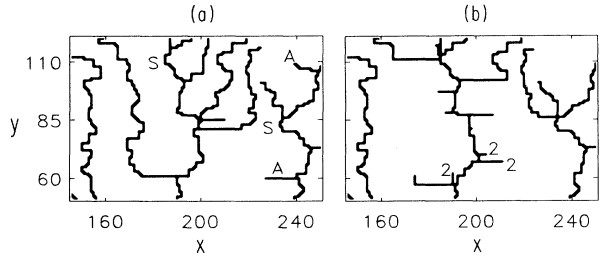

FIG. 3. Details from Figs. 1(e) and 1(f) illustrating changes in the simulated networks with time. In (a) "A" labels streams that will suffer abstraction and "S" marks locations for stream capture. In (b) "2" labels newly formed, second generation branches.

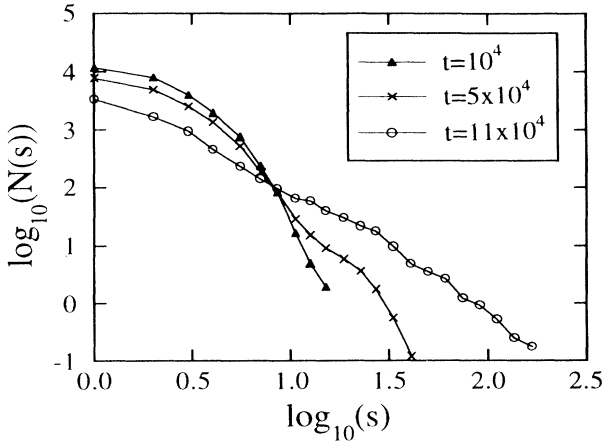

FIG. 4. Histograms of s, the length in steps of the straight line sections that comprise the river networks' main branches (Strahler order >1), at three times in the evolution: ($\triangle$) $t=10^4$ iterations, ($\times$) $t=5\times10^4$ iterations, and ($\circ$) $t=11\times10^4$ iterations. The data are a collection from fourteen 300×200 site simulations generated with the same model parameters that produced Fig. 1 and are compiled in bins spaced equally in logarithmic steps. Each point is the number of straight sections with lengths that fall within its bin divided by bin size. As time progresses, the number of long straight paths increases.

have formed in experimental basins when conditions allow rapid incision of the main valley into the landscape [28]. However, because we typically set $E>1/M$, these second-generation branches align parallel to one another and show little meandering, simulating structures more reminiscent of hillslope runoff than stream segments. In this respect the appearance of these branches reflects a shortcoming in the procedure to identify rivers on the terrain, and their consequence for the statistical properties of model's rivers becomes apparent late in the simulations, as we describe below.

The steady growth of dominant hillslopes, which provide the environment for these second-generation streams, occurs as erosion continues to lower the valley levels. Implementing more complicated, but empirically more physical erosion procedures [31], or alternatively setting a base level below which erosive forces become ineffective, would provide the model with mechanisms which counteract this trend [32]. Also, as we discuss in Sec. III, deposition of avalanched mass acts to mitigate this growth, thus providing a more spatially uniform landscape evolution.

C. Statistical properties of the model networks

Analyzing the simulations' statistical features as they proceed through their evolution, we find that the structure of the simulated networks maintains agreement with statistical properties characteristic of natural river networks. This maintenance of quantitatively correct river network features during a realistic evolutionary process is, we believe, the model's strongest attribute. In the following sections, we discuss several examples of these comparisons.

1. Horton's laws

The hierarchical ordering scheme for the segments of river systems, introduced by Horton [33] and later modified by Strahler [34], has formed the basis for a quantitative description of drainage network morphology. In Strahler's scheme all channels from a head downstream to the first intersection are first-order segments, $u=1$. When two streams of the same order, u, meet, they form a segment with order $u+1$. When two streams of different order meet, the lower-order segment terminates and the downstream channel remains part of the higher-order stream.

Applying this ordering scheme to a natural river network, one finds that the number of segments, $N(u)$, and the mean length of segments, $\langle l(u)\rangle$, of each order follow geometric relations [33]:

$$N(u)\propto\exp(-r_b u)\ , \tag{6a}$$

$$\langle l(u)\rangle\propto\exp(r_l u)\ , \tag{6b}$$

where r_b and r_l are the natural logarithms of the bifurcation and length ratios, R_b and R_l, respectively, $r_b=\ln(R_b)$ and $r_l=\ln(R_l)$. By defining the network's drainage basin as the area of land which receives precipitation that ultimately contributes to the rivers, one finds that the mean areas of basins, $\langle A(u)\rangle$, also follows a geometric relation [26]:

$$\langle A(u)\rangle\propto\exp(r_a u)\ , \tag{6c}$$

where r_a is the natural logarithm of the area ratio, $r_a=\ln(R_a)$.

Using the Strahler ordering scheme, we find that Horton's law of stream numbers, Eq. (6a), holds throughout the simulated river evolution. The inset of Fig. 5(a) gives an example of the number of segments versus order number at one instant in a simulation. r_b evolves with time as shown in Fig. 5(a): it displays a rapid increase to a peak followed by a steady decline. While the long time scales for evolution in nature make direct comparison with this behavior impossible, Abrahams' [35] study of the correlation between decreasing r_b and declining basin relief in a group of natural mature basins provides an indirect measurement of their temporal behavior. Noting that basin relief tends to decrease with age, he identified the correlation as evidence for a reduction in r_b with time during the late stages of basin evolution, similar to the reduction seen in late times in our model.

We also find agreement in the simulations with Eq. (6c), the geometrical relation for mean basin area, when we account for an offset to the basin area that the model introduces. Because the model requires that at least R units flow through any site which is part of a river, basins formed in the simulations have a minimum area of R. Consequently, we modify the law of basin areas as

$$[\langle A(u)\rangle-R]\propto\exp(r_a u) \tag{7}$$

and this form of the law holds well throughout the network evolution [36]. The inset of Fig. 5(b) provides an example of the dependence of $[\langle A(u)\rangle-R]$ on order number, u, at one time in a simulation. The variations in r_a with time, shown in Fig. 5(b), correlate strongly with those of r_b, so that the ratio $2r_b/r_a$, plotted in Fig. 5(c), remains close to 1.8 throughout the evolution. Nikora [37] and Rosso *et al.* [38] calculated this ratio for a large number of river basins. With few exceptions, they found values grouped between 1.6 and 2.0, consistent with the values in the simulations.

The simulations follow the geometrical relation for mean stream length, Eq. (6b), only during the early stage of network development and begin to deviate from it at a time before r_b and r_a have reached their peak values. These deviations occur as the mean length of first-order segments increases disproportionately to that of second order. This growth in the mean length of first-order seg-

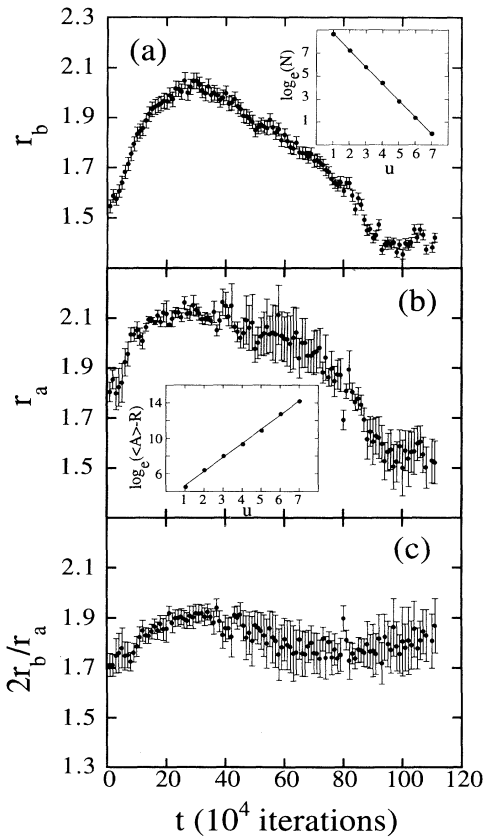

FIG. 5. The time development of r_b and r_a from Horton's laws and of their ratio $2r_b/r_a$. The steady decrease in r_b at late times, shown in (a), matches a trend that measurements suggest exists in natural mature basins [35]. The temporal development of r_a, shown in (b), reveals a strong correlation over time with r_b. The roughly constant ratio, $2r_b/r_a$, in (c) maintains a value consistent with data from natural networks [37,38]. As an example, the inset of (a) shows the scaling of the number of branches, N, with order number u, at $t=90\times10^4$ iterations. The inset of (b) shows the scaling of the mean basin area minus the offset that the model introduces, $(\langle A\rangle-R)$, with u at the same time. The data result from a 1500×1000 site simulation with model parameters: $D=10$, $E=0.05$, $I=1.0$, $M=2000$, and $R=70$.

ments continues throughout the evolution and is consistent with experimental observations of networks that have reached maximum extension [28]. Field measurements also often fail to agree with the law of stream lengths, particularly when Strahler's ordering scheme is applied, and as with the simulations the observed deviations result from excessively long first-order segments [39].

We note that comparison of the simulations with Horton's laws is not a stringent test for the model. Shreve [40] used general statistical arguments to show that the law of stream numbers follows naturally from the ordering procedure in a topologically random assortment of branched networks. In addition, he derived good agreement with the laws of stream lengths and basin areas when he assumed realistic forms for the distributions of lengths and areas that each section of river contributes to a network [39]. However, certain aspects of the simulations, viewed with regard to Horton's laws, such as the *temporal* behaviors of r_b and $2r_b/r_a$ and the systematic deviations from Eq. (6b), indicate a correspondence with nature that extends beyond what one would expect for a topologically random set of branched networks.

2. Hack's law

Aside from Horton's laws, numerous other scaling relations exist among features of river systems. Hack [41] discovered one such characteristic of river network morphology which has become the focus of wide interest [38,42–45]. Defining a principal river in each basin, Hack found that its length scaled with basin area as

$$L_p \propto A^{\alpha} \tag{8}$$

with $\alpha \approx 0.6$ for a group of small drainage systems.

Again, because of the offset introduced to basin areas in the simulations, we modify Hack's law as

$$L_p \propto (A - R)^{\alpha} . \tag{9}$$

We find that this expression holds during the evolution of the drainage networks, where for L_p we use the longest river in each basin. The inset of Fig. 6 shows the scaling of L_p with A at one time in a simulation. Because of the clear deviations from a power law at low L_p, we consider only the behavior for $L_p > 10^2$ in evaluating α. Figure 6 shows the variation of α with time. Initially, while the paths of single units of precipitation on the featureless terrain dictate the resulting river patterns, $\alpha \approx 0.67$, closely matching the value of 0.669 ± 0.001 for the directed-walk model on a square lattice [3]. This result is not surprising since the first units of water transversing the lattice choose among three accessible sites $(x+1,y)$, $(x-1,y)$, $(x,y-1)$ as they perform random walks down the slope, mimicking the rules for the random walks in the directed-walk model [46]. As the landscape evolves, α decreases to a stationary value near $\alpha \approx 0.6$, the value originally measured by Hack. At a more developed stage in the simulations, α decreases from 0.6 to a second stationary value near $\alpha \approx 0.47$. Finally, at very late stages the simulations cease to agree with Hack's law, as the quality of the fits rapidly deteriorates. We associate this failure with the growth of hillslopes to sizes in which second-generation branches, like those shown in Fig. 3(b), enter the calculation of α ($L > 10^2$).

Figure 6 illustrates the behavior of most of the simulations. However, in several simulations α has settled at its second stationary value closer to 0.5 than 0.47. We also note that increasing the lattice size in y, relative to its size in x, can enhance the sharpness of the transition in α between 0.6 and 0.47 [47], indicating that the lateral confinement of the basins on the simulation lattice may play a role in producing this feature.

We have found that the temporal behavior of α in the model corresponds to variations found in nature [19]. Analyzing several thousand data sets, Mueller [48] noted that $\alpha \approx 0.6$ for small basins and that $\alpha \approx 0.5$ for basins with areas between 8000 and 100 000 square miles. He also noted a second rapid change to $\alpha \approx 0.466$ for basins larger than 100 000 square miles. Thus, the early and late stationary values of α in the simulations match those for small and large natural basins, respectively. This correspondence suggests a connection between size and age in drainage basin morphology that has been the subject of criticism [49,50]. However, given the evidence that lateral confinement to the lattice influences the simulations' statistics and the idea that such confinement may at least crudely model constraints on very large basins in nature, we find the association between α as a function of size in nature and as a function of time in the simulations intriguing.

3. Stream length distributions

Recently, the availability of digital elevation maps for large tracts of terrain in the United States has motivated methods for identifying river systems from the structure

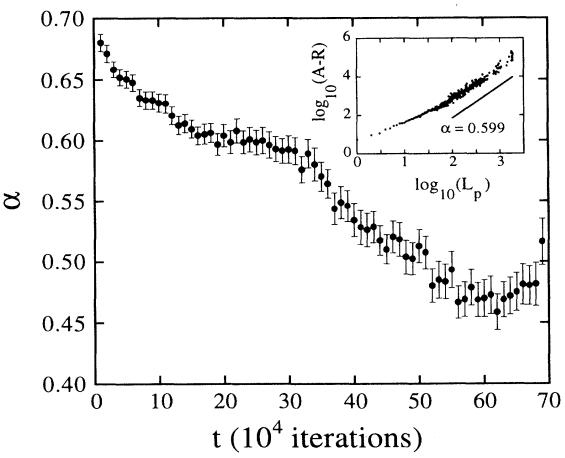

FIG. 6. The time development of the scaling exponent in Hack's law for the same simulation that produced the results in Fig. 5. The stationary values $\alpha = 0.6$ and 0.47 match those values measured for small and large drainage basins, respectively [48]. The inset shows the scaling of the principal river length with basin area at $t = 25 \times 10^4$ iterations.

of natural landscapes. Assigning flow directions between the points on the maps' grids allows the construction of extensive drainage patterns. Studying networks defined on the digital elevation maps, Tarboton *et al.* [51] have fit the length distributions for Strahler segments to a power law at large lengths:

$$N(l > b) \propto b^{-\gamma} \tag{10}$$

with $\gamma \approx 1.8$ to 1.9. At shorter lengths the distributions deviate from this power law, approaching $b = 0$ with nearly zero slope. The simulations produce very similar behavior throughout their evolution. Figure 7 shows the distribution of Strahler lengths at three times in a simulation. At all times the distribution approaches $b = 0$ with nearly zero slope. Initially, a power-law fit at large lengths gives $\gamma \approx 1.5$. At intermediate times, an excess number of long segments appears, creating a bimodal deviation from power-law decay. However, at later times the distribution again fits reasonably to the power-law decay at large lengths with $\gamma \approx 1.9$, the value measured in natural networks. Given the constraints on the simulation data both spatially (with finite size effects entering at large lengths and the rolloff toward $b = 0$ at small) and temporally (with strong deviations at intermediate times), we hesitate to consider the power-law fits as more than a guide. Likewise, the data from the digital elevation maps appear similarly constrained given the limited range of the fits (less than two decades) and the sparseness of data over much of that region [51]. However, the forms of the simulated and natural distributions show strong similarities with one another, particularly at later times in the simulations.

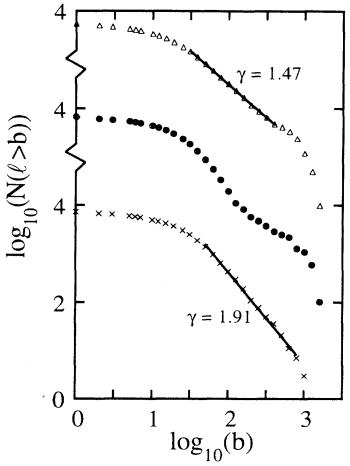

FIG. 7. The distribution of Strahler segment lengths at three times in the same simulation that produced Fig. 5: (△) $t = 5 \times 10^4$ iterations, (●) $t = 40 \times 10^4$ iterations, and (×) $t = 70 \times 10^4$ iterations. The distributions at $t = 5 \times 10^4$ iterations and $t = 40 \times 10^4$ iterations have been offset for clarity. At early and late times the distribution at large lengths approximates a power-law decay with scaling exponent $\gamma \approx 1.5$ at early times and $\gamma \approx 1.9$ at late times. At intermediate times, such as $t = 40 \times 10^4$ iterations, the distribution deviates from this behavior. The late time distribution with $\gamma \approx 1.9$ shows quantitative agreement with data obtained from digital elevation maps [51].

4. *Link length distributions*

Field measurements have revealed that the lengths of external links (first-order Strahler segments) and internal links (pieces of higher-order segments) in natural river networks follow either log-normal distributions [26,52] or gamma distributions [8,37,53]. Figures 8 and 9 display the distributions of external and internal link lengths, respectively, at two times in the evolution. For the external links, while some simulations have suggested that the gamma distribution offers a better description, the data do not indicate that either form is superior during any extended stage in the evolution. The internal link lengths, on the other hand, clearly follow the gamma distribution at early times. At late times the formation of second-generation branches, subdividing the main branches into progressively smaller links, moves the peak in the internal link length distribution to lower values. While the functional forms continue to hold at these late times, as Fig. 9(b) illustrates, this abundance of short links caused by the second-generation tributaries in the simulations represents a deviation from natural distributions.

5. *Area distributions*

Rodríguez-Iturbe *et al.* [54], also using digital elevation maps, fit a power-law distribution to the area drained through each link of a network:

$$N(A > m) \propto m^{-\beta}, \tag{11}$$

where $\beta \approx 0.43$. Figure 10 shows the distribution of drainage areas at three times in a simulation [55]. Be-

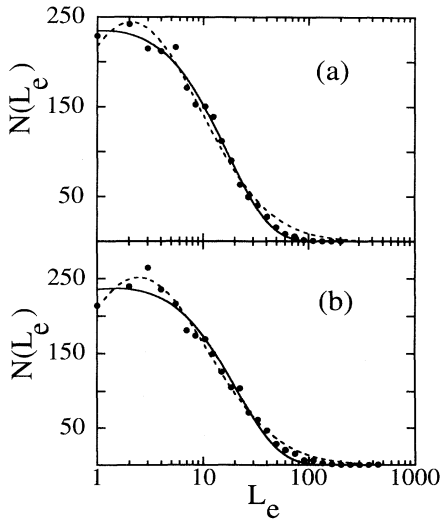

FIG. 8. The distribution of external link lengths, L_e, at two times in a 1500×1000 site simulation: (a) $t = 5 \times 10^4$ iterations and (b) $t = 60 \times 10^4$ iterations. The solid (dashed) lines are fits to a gamma (log normal) distribution. The model parameters used in the simulation were $D = 10$, $E = 0.05$, $I = 1.0$, $M = 2000$, and $R = 70$.

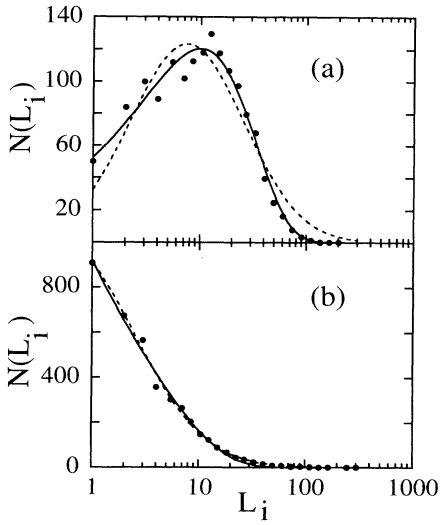

FIG. 9. The distribution of internal link lengths, L_i, at two times in the same simulation that produced Fig. 8: (a) $t=5\times10^4$ iterations and (b) $t=60\times10^4$ iterations. The solid (dashed) lines are fits to a gamma (log normal) distribution.

cause the finite lattice size leads to a sharp deviation from any power law at large basin area, we fit the distributions only for $m<10^4$. As the simulations evolve, β increases from $\beta\approx0.38$ (close to the result of the directed-walk model, $\beta=0.35$[3]) to $\beta\approx0.42$ (a value closer to the result from the digital elevation maps). Small but reproducible curvatures exist in log-log representations of these early time distributions. These curvatures grow at later stages of evolution, as the entire landscape becomes dominated by the hillslopes of a few large basins. Data from the latest time in Fig. 10 show such a distribution. During the period in which power-law fits seem reasonable, however, the scaling exponent β approaches the one measured from the digital elevation maps.

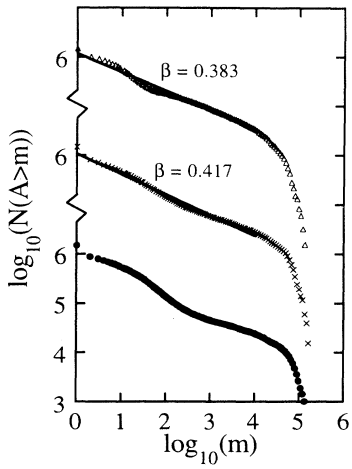

FIG. 10. The distribution of drainage areas, A, for all sites at three times in the same simulation that produced Fig. 8: (△) at $t=1\times10^4$ iterations, (×) at $t=15\times10^4$ iterations, and (●) at $t=30\times10^4$ iterations. The distributions at $t=1\times10^4$ iterations and $t=15\times10^4$ iterations have been offset for clarity. At early times power-law scaling provides a good description of the distribution with the scaling exponent approaching with time $\beta=0.43$, the value measured from digital elevation maps [54]. Deviations from the power-law scaling become pronounced at later times.

6. *Energy optimization*

We have also analyzed the changing morphology of the model networks in terms of the energy expenditure criteria postulated by Rodríguez-Iturbe *et al.* [12]. According to these criteria branches configure themselves to minimize the network's total power loss, given by

$$P \propto \sum L_j A_j^{0.5} , \tag{12}$$

where the sum is over all links in the network, and L_j and A_j are the length and drainage area of the jth link. Figure 11 shows $P(t)/P(t=500)$ averaged over 40 separate 300×200 networks, with $R=100$ and $R=200$. As the networks evolve from their initial random-walk patterns, their energy expenditure, as expressed by Eq. (12), decreases. Thus, the evolution of this early period drives the system toward an optimal state as viewed by Rodríguez-Iturbe *et al.* However, for smaller R the total power increases at later times. We identify this increase with the formation of second-generation branches on large hillslopes. As discussed by Rigon *et al.* [56], such straight, parallel flow, characteristic of hillslope runoff, should not optimize Eq. (12).

III. MASS CONSERVING MODEL

The avalanche scheme plays the central role in producing the temporal changes in the simulated landscapes.

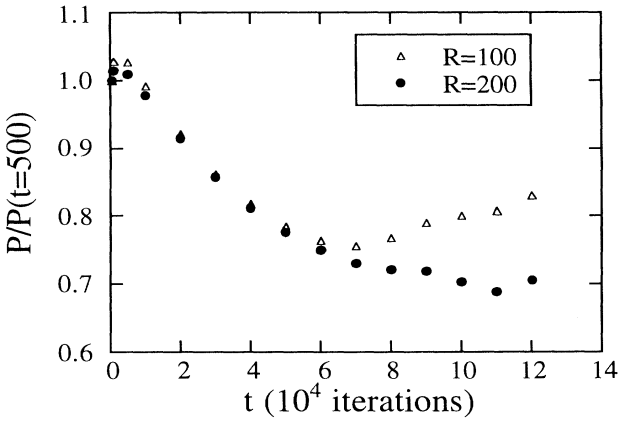

FIG. 11. The variation with time of the total power loss, P, as defined by Eq. (13), normalized to the power loss after 500 iterations. The data, compiled from forty 300×200 site simulations with model parameters $D=10$, $E=0.05$, $I=1.0$, $M=2000$, are for two values of the threshold parameter: (△) $R=100$ and (●) $R=200$. The steady decrease in power loss with time indicates that the evolving networks are approaching an optimal configuration, as described by Rodríguez-Iturbe *et al.* [12]. The increase at late times for $R=100$ reflects the contributions to the networks of second-generation tributaries on the hillslopes.

Therefore, we have varied the way the avalanches occur in the model to test the sensitivity of the evolution to their precise form. The simulations with this modified model follow the same iterative procedure outlined in Sec. II A, except that Eq. (5) in step (iv) is replaced by

$$h(x_h,y_h)\rightarrow h(x_h,y_h)-\Delta h/8\ , \tag{13a}$$

$$h(x_l,y_l)\rightarrow h(x_l,y_l)+\Delta h/8\ , \tag{13b}$$

thereby conserving the avalanched soil by redistributing it to the low side, (x_l,y_l), of the steep slope.

This alteration in the model introduces the complication that local minima form in the interior of the lattice from which the probability distribution, Eq. (3), makes no allowance for escape. Therefore, when Eq. (3), with the proviso that the water not return to the site it immediately vacated, leads to zero probability of movement in all directions, the water automatically flows from the occupied site in the same direction as the last unit of precipitation to visit that site. In the escape of a minimum, this rule leads to flow to a site of higher elevation. When recording the erosive effects of the water in step (iii), the model does not apply Eq. (4) to those sites from which the flow is uphill, so that the erosion of subsequent precipitation quickly removes any local minima formed upstream of avalanched soil. Occasionally (less than 1% of all iterations), the water enters a pathologically configured minimum for which this escape procedure fails. In such cases the water follows the path of its immediate predecessor not only out of the minimum but to the edge of the lattice, $y=0$. Again, because sites from which the flow is uphill do not erode, these pathologies are short lived. The definition of the rivers is the same in this model as for the non-mass conserving model with the stipulation that, if a test unit enters a minimum, it leaves following the direction of the last eroding precipitation to visit the site.

In choosing parameter values for simulations with this version of the model we followed the same procedures described in Sec. II A. However, we typically used a smaller value of M, while maintaining $M>D$, to limit the size of barriers forming minima in the landscape. Also, we moved $\Delta h/8$ units in the avalanche scheme so that the relative change in slope after an avalanche matched that in the simulations with the non-mass-conserving model.

Figures 12(a)–12(c) show an evolving terrain simulated with the mass conserving model. Comparison with Fig. 1 reveals qualitative differences between these landscapes and those formed using the non-mass-conserving model. Both simulations begin with V-shaped valleys initiating at $y=0$. However, this formative stage comprises a much smaller fraction of the total time of evolution when avalanched mass is redeposited. In simulations with the non-mass-conserving model, the valleys quickly broaden near their mouths, so that the region near $y=0$ becomes dominated by a few large basins before the terrains' upper reaches suffer any significant erosion. In contrast, when avalanched soil replenishes the valley bottoms, the headward growing valleys fill the landscape before the region near $y=0$ reaches more advanced stages of erosion. These two morphologies represent two extremes with respect to the ability of the river system to transport avalanche debris. In the original model the rivers can fully support the instantaneous removal of avalanched mass. In the mass conserving model, however, this sedimentation erodes no more easily than the undetached terrain beneath. These differences provide an example of the effect a conserved variable introduces to the dynamics in the simulations.

Despite these differing landscape features, the river networks created in the mass conserving model, shown in Figs. 12(d)–12(h), have the same general features as those in Fig. 1. In particular, the dominant characteristics of their evolution remain: abstraction and stream capture as well as the straightening of main branches and the growth of second-generation streams at late times. How-

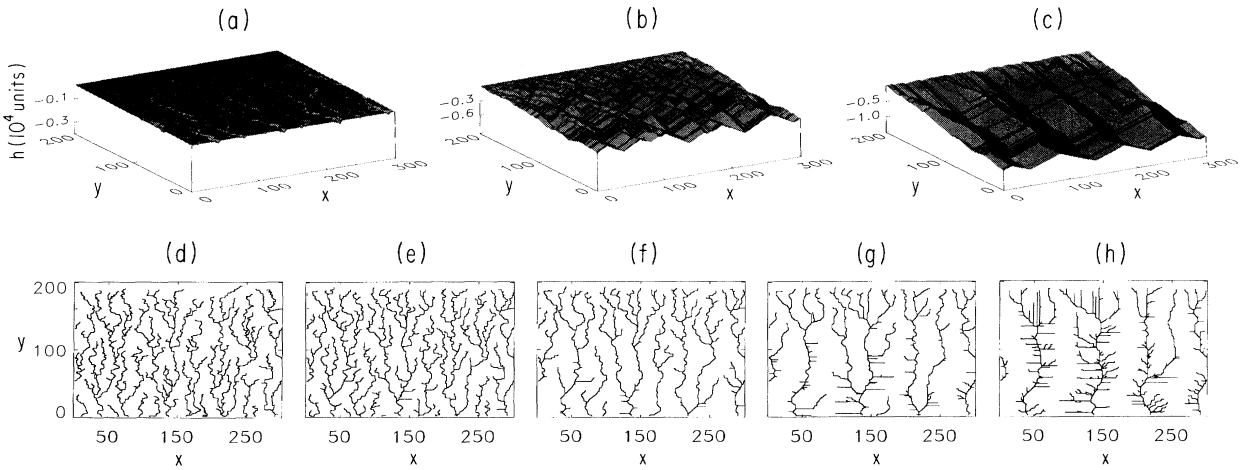

FIG. 12. The evolution of a landscape: (a) $t=400$ iterations, (b) $t=4\times10^4$ iterations, and (c) $t=25\times10^4$ iterations; and corresponding river networks: (d) $t=400$ iterations, (e) $t=1\times10^4$ iterations, (f) $t=4\times10^4$ iterations, (g) $t=10\times10^4$ iterations, and (h) $t=25\times10^4$ iterations, produced by the mass conserving model. The model parameters used in the 300×200 site simulation were $D=10$, $E=0.05$, $I=1.0$, $M=80$, and $R=100$.

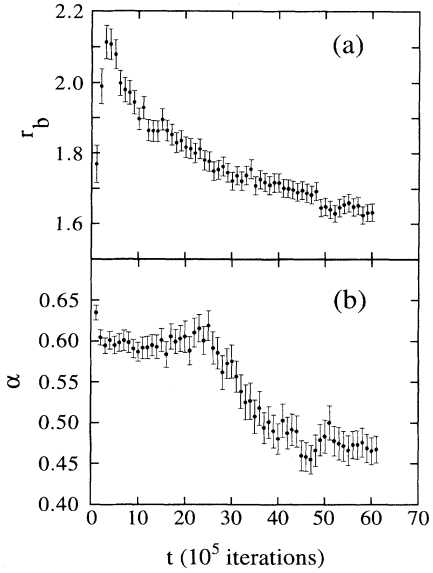

FIG. 13. The time developments of r_b from Horton's law, shown in (a), and α from Hack's law, shown in (b), for a 1200×1000 site simulation produced with the mass conserving model. The model parameters used were $D=10$, $E=0.05$, $I=1.0$, $M=80$, and $R=70$. The variations in time of these statistical features repeat the behavior seen in the non-mass-conserving model, shown in Figs. 5(a) and 6, although over a greatly extended time scale.

ever, because the mass conserving model produces a more spatially uniform valley development, its simulations do not share the pronounced temporal overlap of the headward invasion of valleys and the abstraction of tributaries that the non-mass-conserving model displays.

The statistical properties of river networks produced with each model reveal slightly different temporal behavior, reflecting the differences in the landscape evolution. Figures 13(a) and 13(b) show the variation with time of r_b from Horton's law and α from Hack's law, respectively, in a simulation produced with the mass conserving model. Compared with the original model the rapid increase in r_b and decrease from 0.67 to 0.6 in α comprise a much smaller portion of the total time of evolution. However, the exponents vary in the same general manner as they do in simulations with the non-mass-conserving model: r_b shows a steady decrease during most of the evolution and α has two stationary values near 0.6 and 0.47. Indeed, we have repeated our analysis for the mass conserving model of all of the statistical properties of river networks described in Sec. II C and have found that, despite the differences in landscape features, the behavior for each property shows agreement with the original model.

IV. CONCLUSION

In the sections above we have stressed the correspondence between the spatial and temporal features of the simulations and those observed in nature. Despite these successes we note that the model may serve less as a concise enumeration of mechanisms driving network evolution than as a warning about the ease of producing branches structures that possess certain statistical characteristics. As Shreve demonstrated for Horton's laws, many bifurcating branched networks could, as a general property of their form, possess statistical properties that are considered distinguishing characteristics of river networks. However, a noteworthy attribute of the models' performance is that the simulated networks improve their compliance with several statistical features, such as Hack's law and the stream length and area distributions, as they evolve from their initial configuration of random-walk aggregates. Thus, with only simple procedures for erosion and avalanching, the model produces a realistic evolution that maintains or improves the networks' agreement with natural river systems.

Finally, along with its successes the model's limitations may offer insight, particularly when the missing elements that would extend its correspondence with natural systems can be identified. For example, the use of the threshold parameter, R, in defining the rivers, while an extremely simple criterion to implement, results in network extension incommensurate with the degree of erosion at early times and introduces second-generation tributaries on large hillslopes which adversely effect some statistical features at late times. Current research to improve methods of locating rivers on digital elevation maps [57] may prove helpful in the definition of rivers in lattice simulations which avoid these problems. In addition, only with a more realistic description of the transport and sedimentation of soil eroded via Eq. (4) could we hope to compare some of the statistical properties of the simulated terrains against natural features, such as the variation of stream gradient with drainage area [58] or the roughness of the erosional landscapes [18,59]. Given the simplicity of the model in its present form, the breadth of comparisons we have been able to make in both its temporal and statistical behavior with natural river networks provides encouragement for future work.

ACKNOWLEDGMENTS

I am grateful to Sid Nagel, with whom I worked in close consultation throughout this project, for his support and guidance. Funding was provided by NSF Grant No. DMR 94-10478 and DOE Grant No. DE-FG02-92ER25119.

[1] L. B. Leopold and W. B. Langbein, U.S. Geol. Surv. Prof. Paper **500A**, 1 (1962).
[2] A. E. Scheidegger, Int. Assoc. Sci. Hydro. Bull. **12**, 15 (1967).
[3] P. Meakin, J. Feder, and T. Jøssang, Physica **A176**, 409 (1991).
[4] I. Seginer, Water Resour. Res. **5**, 591 (1969).
[5] J. S. Smart and V. L. Moruzzi, J. Geol. **79**, 572 (1971).
[6] A. D. Howard, Geogr. Anal. **3**, 29 (1971).
[7] A. D. Howard, Geol. Soc. Am. Bull. **82**, 1355 (1971).

[8] D. L. Dunkerley, J. Geol. **85**, 459 (1977).
[9] C. P. Stark, Nature **352**, 423 (1991).
[10] A. D. Abrahams, Water Resour. Res. **20**, 161 (1984).
[11] A. D. Howard, Water Resour. Res. **26**, 2107 (1990).
[12] I. Rodríguez-Iturbe, A. Rinaldo, R. Rigon, R. L. Bras, A. Marani, and E. Ijjasz-Vasquez, Water Resour. Res. **28**, 1095 (1992).
[13] A. Rinaldo, I. Rodríguez-Iturbe, R. Rigon, E. J. Ijjasz-Vasquez, and R. L. Bras, Phys. Rev. Lett. **70**, 822 (1993).
[14] H. Inaoka and H. Takayasu, Phys. Rev. E **47**, 899 (1993).
[15] G. R. Willgoose, R. L. Bras, and I. Rodríguez-Iturbe, Am. Geophys. Union Trans. **71**, 1806 (1990).
[16] G. R. Willgoose, R. L. Bras, and I. Rodríguez-Iturbe, Water Resour. Res. **27**, 1685 (1991).
[17] A. D. Howard, Water Resour. Res. **30**, 2261 (1994).
[18] A. Czirok, E. Somfai, and T. Vicsek, Phys. Rev. Lett. **71**, 2154 (1993).
[19] R. L. Leheny and S. R. Nagel, Phys. Rev. Lett. **71**, 1470 (1993).
[20] C. G. Chase, Geomorphology **5**, 39 (1992).
[21] K. M. Gregory and C. G. Chase, Geophys. Res. **99**, 20 141 (1994).
[22] This procedure resembles that developed to identify networks on digital elevation maps of natural terrains; see J. F. O'Callaghan and D. M. Marks, Comput. Vision Graphics Image Process. **28**, 323 (1984).
[23] W. S. Glock, Geograph. Rev. **21**, 475 (1931).
[24] R. J. Small, *The Study of Landforms* (Cambridge University Press, New York, 1978).
[25] See, e.g., R. V. Ruhe, Am. J. Sci. **250**, 46 (1952).
[26] S. A. Schumm, Geol. Soc. Am. Bull. **67**, 597 (1956).
[27] M. Morasawa, Am. J. Sci. **262**, 340 (1964).
[28] S. A. Schumm, M. P. Mosley, and W. E. Weaver, *Experimental Fluvial Geomorphology* (Wiley, New York, 1987).
[29] M. A. Carson and D. J. Petley, Trans. Inst. Brit. Geogr. **49**, 71 (1970).
[30] M. A. Carson, Inst. Brit. Geogr. Spec. Publ. **3**, 31 (1971).
[31] A. D. Howard, W. E. Dietrich, and M. A. Seidl, Geophys. Res. **99**, 13 971 (1994), and reference therein.
[32] As a first approximation to such a model, we have introduced to the rules a minimum height to simulate the presence of a bedrock or a base level, below which erosion via Eq. (4) ceases. Preliminary results indicate that this assumption generates interesting changes in landscape features; R. L. Leheny and S. R. Nagel (unpublished).
[33] R. E. Horton, Geol. Soc. Am. Bull. **56**, 275 (1945).
[34] A. N. Strahler, Geol. Soc. Am. Bull. **63**, 1117 (1952).
[35] A. D. Abrahams, Water Resour. Res. **8**, 624 (1972).
[36] Field observations, which show a threshold length for overland flow before channels form [see, for example, D. R. Montgomery and W. E. Dietrich, Science **225**, 826 (1992)], suggest that subtracting R in the simulations should be unnecessary. We note, however, that this correction effects only small basins and becomes negligible for $A \gg R$.
[37] V. I. Nikora, Water Resour. Res. **30**, 133 (1994).
[38] R. Rosso, B. Bacci, and P. La Barbera, Water Resour. Res. **27**, 381 (1991).
[39] R. L. Shreve, J. Geol. **77**, 397 (1969).
[40] R. L. Shreve, J. Geol. **74**, 17 (1966).
[41] J. T. Hack, U.S. Geol. Surv. Prof. Paper **294B**, 45 (1957).
[42] O. J. Mesa and V. K. Gupta, Water Resour. Res. **23**, 2119 (1987).
[43] R. S. Snow, in *Fractal in Geophysics,* edited by C. H. Scholz and B. B. Mandelbrot (Birkhauser Verlag, Boston, 1989), p. 100.
[44] A. Robert and A. G. Roy, Water Resour. Res. **26**, 839 (1990).
[45] E. J. Ijjasz-Vasquez, R. L. Bras, and I. Rodríguez-Iturbe, Geophys. Res. Lett. **20**, 1583 (1993).
[46] Strictly, the model's early precipitation follows rules matching the directed walk model only in the limit $D \ll I \ll 1/E$; however, the initial value of α appears independent of D/I.
[47] Compare, for example, Fig. 6 with Fig. 3 of [19].
[48] J. E. Mueller, Geol. Soc. Am. Bull. **84**, 3127 (1973).
[49] M. P. Mosley and R. S. Parker, Geol. Soc. Am. Bull. **83**, 3669 (1972).
[50] M. P. Mosley and R. S. Parker, Geol. Soc. Am. Bull. **84**, 3123 (1973).
[51] D. G. Tarboton, R. L. Bras, and I. Rodríguez-Iturbe, Water Resour. Res. **24**, 1317 (1988).
[52] A. N. Strahler, J. Geol. **62**, 1 (1954).
[53] J. J. Smart, Adv. Hydrosci. **8**, 305 (1972).
[54] I. Rodríguez-Iturbe, E. J. Ijjasz-Vasquez, R. L. Bras, and D. G. Tarboton, Water Resour. Res. **28**, 1089 (1992).
[55] To construct the distributions we use every site on the landscape. However, we find that this procedure and that used in [54] lead to identical distributions for our data, except at late times when the increased importance of second-generation branches disproportionate weight to links of large area.
[56] R. Rigon, A. Rinaldo, I. Rodríguez-Iturbe, R. L. Bras, and E. Ijjasz-Vasquez, Water Resour. Res. **29**, 1635 (1993).
[57] See, for example, D. G. Tarboton, R. L. Bras, and I. Rodríguez-Iturbe, Hydro. Proc. **5**, 81 (1991).
[58] J. J. Flint, Water Resour. Res. **10**, 969 (1974).
[59] G. Dietler and Y. Zhang, Physica A **191**, 213 (1992).

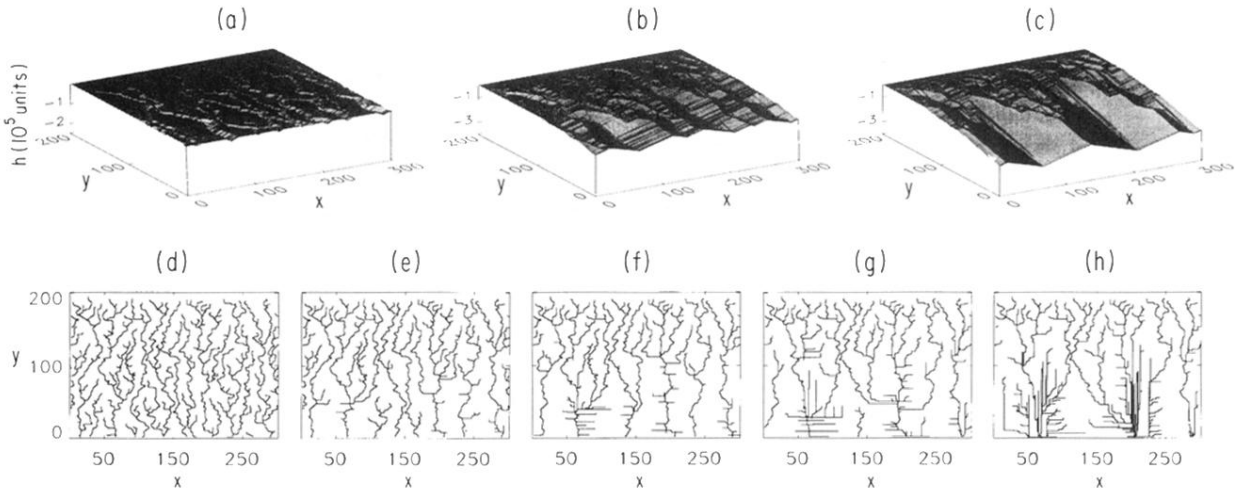

FIG. 1. The evolution of the landscape: (a) at $t=1\times10^4$ iterations, (b) at $t=5\times10^4$ iterations, and (c) at $t=9\times10^4$ iterations; and the corresponding river networks (d) at $t=1\times10^4$ iterations, (e) at $t=3\times10^4$ iterations, (f) at $t=5\times10^4$ iterations, (g) at $t=7\times10^4$ iterations, (h) at $t=9\times10^4$ iterations, in a 300×200 site simulation. The model parameters were $D=10$, $E=0.05$, $I=1.0$, $M=2000$, and $R=100$.

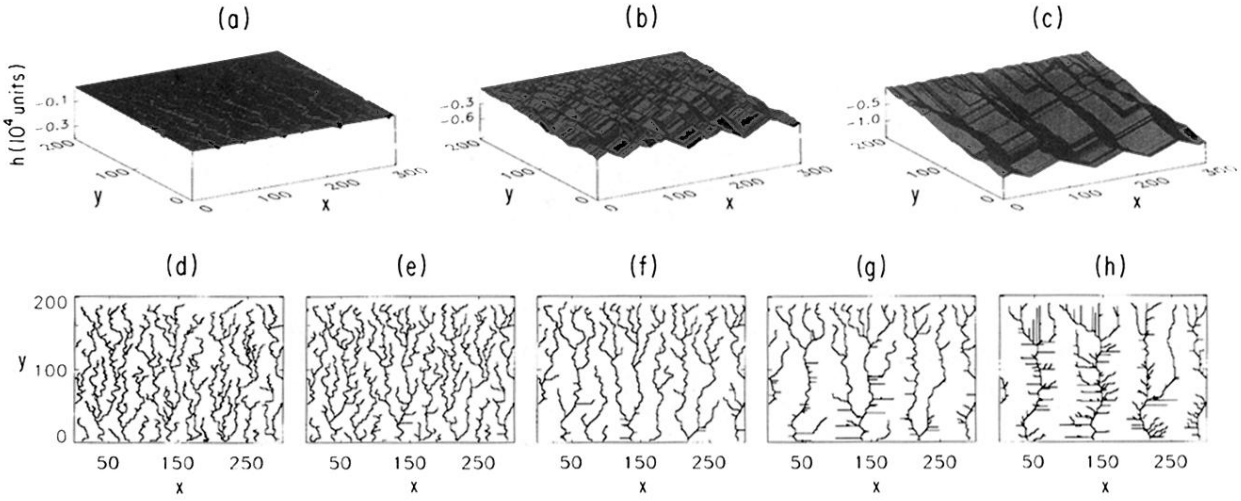

FIG. 12. The evolution of a landscape: (a) $t=400$ iterations, (b) $t=4\times10^4$ iterations, and (c) $t=25\times10^4$ iterations; and corresponding river networks: (d) $t=400$ iterations, (e) $t=1\times10^4$ iterations, (f) $t=4\times10^4$ iterations, (g) $t=10\times10^4$ iterations, and (h) $t=25\times10^4$ iterations, produced by the mass conserving model. The model parameters used in the 300×200 site simulation were $D=10$, $E=0.05$, $I=1.0$, $M=80$, and $R=100$.